Single-Molecule Force Spectroscopy from Nanodiscs: An Assay to Quantify Folding, Stability, and Interactions of Native Membrane Proteins

Michael Zocher,[†,‡] Christian Roos,[§] Susanne Wegmann,[†] Patrick D. Bosshart,[†] Volker Dötsch,[§] Frank Bernhard,[§] and Daniel J. Müller[†,*]

[†]Biosystems Science and Engineering (BSSE), ETH Zürich, Mattenstraße 26, 4058 Basel, Switzerland, [‡]M.E. Müller Institute for Structural Biology, Biozentrum, University of Basel, Klingelbergstraße 70, 4056 Basel, Switzerland, and [§]Institute of Biophysical Chemistry, Goethe University Frankfurt, Max-von-Laue-Straße 9, 60438 Frankfurt/Main, Germany

ABSTRACT Single-molecule force spectroscopy (SMFS) can quantify and localize inter- and intramolecular interactions that determine the folding, stability, and functional state of membrane proteins. To conduct SMFS the membranes embedding the membrane proteins must be imaged and localized in a rather time-consuming manner. Toward simplifying the investigation of membrane proteins by SMFS, we reconstituted the light-driven proton pump bacteriorhodopsin into lipid nanodiscs. The advantage of using nanodiscs is that membrane proteins can be handled like water-soluble proteins and characterized with similar ease. SMFS characterization of bacteriorhodopsin in native purple membranes and in nanodiscs reveals no significant alterations of structure, function, unfolding intermediates, and strengths of inter- and intramolecular interactions. This demonstrates that lipid nanodiscs provide a unique approach for *in vitro* studies of native membrane proteins using SMFS and open an avenue to characterize membrane proteins by a wide variety of SMFS approaches that have been established on water-soluble proteins.

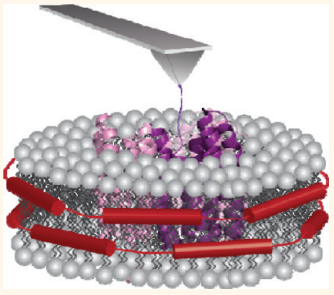

KEYWORDS: AFM · atomic force microscopy · bacteriorhodopsin · circular dichroism · DMPC · membrane scaffold protein 1 · purple membrane · reconstitution · SMFS · unfolding intermediates · unfolding pathways

Membrane proteins play important roles in life. They are responsible for energy conversion, generate and maintain ion gradients, synthesize fuel molecules, transduce signals, recognize molecules, facilitate cell adhesion, and contribute to virtually every fundamental cell biological process.[1] Membrane proteins that are encoded by 20–30% of the open reading frames from archaebacterial, bacterial, and eukaryotic organisms[2] must fold into well-defined three-dimensional structures to fulfill their delicate functional tasks. To understand the principles of how membrane proteins fold into their functional structure and how these structures are stabilized, destabilized, and functionally modulated by inter- and intramolecular interactions is one of the major challenges in biology.[3–7] However, biophysical studies quantifying these properties of membrane proteins *in vitro* remain an intricate task. These difficulties are based on the amphiphilic character of membrane proteins that once isolated from the cell membrane must be reconstituted into a lipid bilayer that mimics the native cellular membrane.

Recently, phospholipid nanodiscs have been introduced to reconstitute membrane proteins into a native-like lipid environment.[8–10] Nanodiscs are composed of small patches (≈10–20 nm in diameter) of a lipid bilayer that is framed by the amphiphilic membrane scaffold protein to shield the hydrophobic fatty acid chains of the lipids from the aqueous buffer solution. This shielding of hydrophobic interactions makes lipid nanodiscs water-soluble. Therefore, after integration into nanodiscs, membrane proteins can be handled similarly to water-soluble proteins. Because the length of the membrane scaffold protein determines the diameter of the nanodisc and the lipid composition of the nanodisc can be adjusted, the properties of the nanodisc can be tailored to favor the insertion of a particular membrane protein.[10] Accordingly, several membrane proteins could be embedded into lipid nanodiscs including the bacterial chemoreceptor Tar,[11] cytochrome P450,[12] the translocon SecYEG,[13] bacteriorhodopsin,[14] the human β_2-adrenergic receptor,[15,16] and bovine rhodopsin.[17] Structural and functional characterization of these membrane proteins demonstrated

* Address correspondence to daniel.mueller@bsse.ethz.ch.

Received for review November 28, 2011 and accepted December 25, 2011.

Published online December 25, 2011
10.1021/nn204624p

that nanodiscs mimic a physiological environment for *in vitro* studies.[11,18−21]

Atomic force microscopy (AFM)-based single-molecule force spectroscopy (SMFS) offers the opportunity to study the folding and the unfolding pathways of membrane proteins.[22,23] When unfolding a membrane protein, SMFS can further quantify inter- and intramolecular interactions in the piconewton range and locate these interactions on the primary, secondary, or tertiary structure of the membrane protein.[22] It was shown that the (un)folding pathways and the interactions of membrane proteins depend on subtle changes of the environment such as temperature,[24] electrolyte,[25−27] pH of the buffer solution,[25] or the oligomeric state[28] of the membrane protein. Other examples used SMFS to detect and structurally locate the interactions established upon ligand and inhibitor binding,[25,27,29−31] inserting mutations,[32,33] and changing the functional state[25,27,34] of the membrane protein. To reveal these insights by SMFS requires the membrane protein to be embedded in a lipid membrane. These membranes can be extracted from the native cell or synthetic lipid membranes into which the membrane protein has been reconstituted. In contrast to the thousands of different membrane proteins known, only a few could be reconstituted into the functionally important lipid membrane.[9,35,36]

Another bottleneck limits the applicability of SMFS to membrane proteins. To conduct SMFS, the protein-containing membrane must be first imaged by AFM and located so that the AFM tip can be attached to the membrane protein. Once the AFM tip has been attached, the stability, folding, and interactions of the membrane protein can be characterized.[22,23,37] Simply increasing the density of membranes covering the sample support is often not useful to circumvent the need of AFM imaging. The reason is that if adsorbed at higher concentration onto the support, protein membranes start forming aggregates, which is not favorable for SMFS. These constraints could be avoided if membrane proteins are reconstituted into lipid nanodiscs that render membrane proteins hydrophilic and nanoscopic. Dense adsorption layers on sample supports can be prepared with hydrophilic water-soluble proteins,[38] and in principle dense adsorption layers should be obtainable using membrane proteins that are embedded in hydrophilic nanodiscs. In a raster-like manner the AFM tip could then pick up and characterize one membrane protein after the other without the need of imaging. Such improved preparation procedures would simplify SMFS of membrane proteins and be a basis to apply high-throughput SMFS assays[39,40] to study membrane protein (un)folding, stability, and interactions.

For these reasons, we investigate whether membrane proteins reconstituted into phospholipid nanodiscs can be characterized by SMFS and to what extent the reconstitution into nanodiscs modulates the interactions guiding the stability and (un)folding of membrane proteins. Among membrane proteins the light-driven proton pump bacteriorhodopsin (BR) from *Halobacterium salinarum* most probably represents the functionally and structurally best characterized example.[41−44] Moreover, for many years BR serves as a model to characterize the unfolding and folding of α-helical transmembrane proteins.[37,45−48] Thus, we have chosen BR as an example for our studies and characterized BR from native purple membrane (BR_{PM}) and BR reconstituted into phospholipid nanodiscs (BR_{ND}) by SMFS. The mechanical unfolding pathways and the stability of both BR samples are compared, and their interactions mapped onto the BR structure. The results teach us whether the reconstitution of BR into lipid nanodiscs alters the properties of BR and whether nanodiscs can in principle be applied to characterize membrane proteins by SMFS.

RESULTS AND DISCUSSION

Mechanically Unfolding Single BR Molecules from Purple Membrane and from Nanodiscs. After reconstituting BR into dimyristoylphosphatidylcholine (DMPC) lipid nanodiscs we recorded absorption spectra of BR in native purple membrane (BR_{PM}) and of BR in nanodiscs (BR_{ND}) (Figure S1, SI). BR_{PM} and BR_{ND} showed similar absorption spectra between 450 and 650 nm that are characteristic for the native light-driven proton pump BR.[49] Thus, we conclude that reconstitution into lipid nanodiscs did not change the functional properties of BR significantly. We used circular dichroism (CD) to determine the assembly of BR in nanodiscs.[50,51] The CD spectra of BR_{ND} showed peaks in the visible spectrum from 400 to 700 nm (Figure S2, SI) that are typical for trimeric BR.[52] Consequently, BR trimers were reconstituted into lipid nanodiscs.

For SMFS native purple membrane (BR_{PM}) or BR_{ND} was adsorbed to mica and imaged by AFM in buffer solution (Figure S3, SI).[38] Whereas purple membranes were heterogeneously distributed over the supporting mica, the BR_{ND} complexes were homogeneously distributed and densely packed. To attach a single BR *via* unspecific interactions to the AFM tip,[37] the tip was brought into contact with the sample (BR_{PM} or BR_{ND}) applying a force of ∼1 nN for 1 s. In ∼0.5% (BR_{PM}, $n \approx 20.000$) or ∼0.05% (BR_{ND}, $n \approx 250.000$) of all cases a single BR molecule attached with its terminal end to the AFM tip (Figure 1). Withdrawal of the AFM tip stretched and stressed the terminal end and induced the unfolding of BR.[37] The force−distance (F−D) curve recorded during withdrawal of the AFM tip showed a characteristic sawtooth-like pattern (Figure 2a,b) that has been assigned to the mechanical unfolding of BR from the C-terminal end.[37,53]

In our experiments, BR molecules could attach unspecifically *via* either the N-terminal or the C-terminal end to the AFM tip (Methods). As reported earlier the F−D curves showed a specific pattern depending from

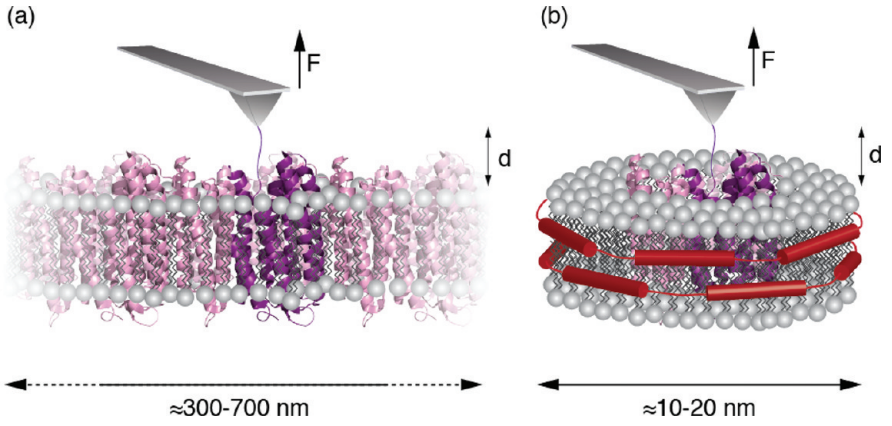

Figure 1. Schematic representation of SMFS of bacteriorhodopsin (BR) embedded in native purple membrane (BR_{PM}) and lipid nanodiscs (BR_{ND}). (a) and (b) are illustrations of BR trimers embedded in purple membrane (BR_{PM}) and in a lipid nanodisc (BR_{ND}), respectively. After attachment of the AFM tip to the C-terminal end of a single BR molecule, the AFM tip is withdrawn to apply mechanical stress to the membrane protein. A force–distance (F–D) curve records the deflection of the AFM cantilever as a function of the distance (d) between AFM tip and membrane (Figure 2a,b). F–D curves recorded for BR_{PM} and BR_{ND} show that sufficiently high mechanical stress induces stepwise unfolding of the membrane protein.

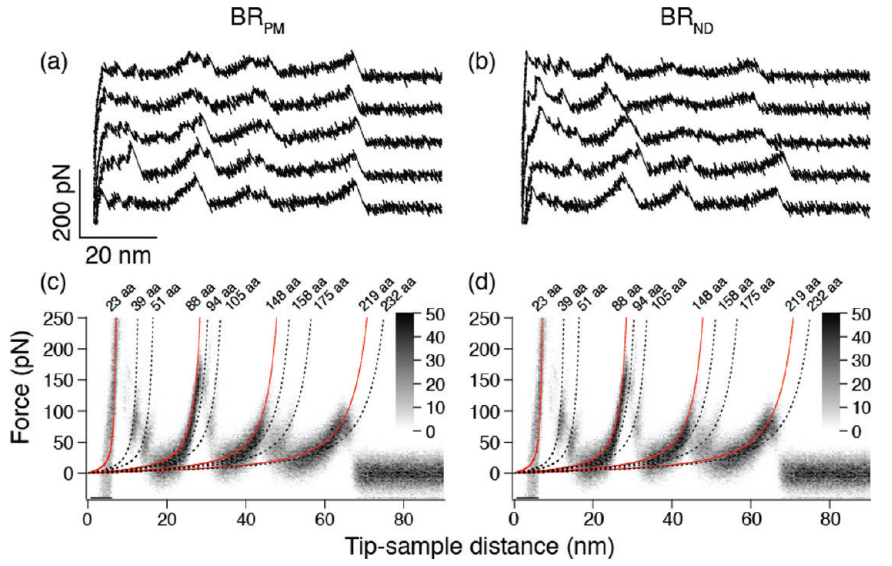

Figure 2. Mechanical unfolding of bacteriorhodopsin in native purple membrane and in lipid nanodiscs. Selection of F–D curves that record the unfolding of single BR_{PM} (a) and BR_{ND} (b) molecules. Every force peak of every F–D curve detects an unfolding intermediate of BR with all force peaks (unfolding intermediates) describing the unfolding pathway taken by an individual BR molecule. Superimpositions of 100 F–D curves recorded for BR_{PM} (c) and BR_{ND} (d). Red lines are WLC curves fitting the main force peaks that occur at a probability of 100%, whereas black dashed lines are worm-like chain (WLC) fits of minor force peaks that occur at probability <80%. The numbers next to each WLC curve assign the contour length (given in amino acids (aa) for every fit) of a force peak. This contour length approximates the length of the unfolded and stretched polypeptide. Gray scale bars allow evaluating how frequently individual force peaks were populated.

which terminal end BR was unfolded.[54] However, the probability of the N-terminal end of attaching to the AFM tip was much lower than that of the C-terminal end.[37,54] Thus, for statistical reasons we analyzed only F–D curves that reflected the unfolding of BR from the C-terminal end. The mechanical unfolding of BR from the C-terminal end can be described as follows:[37,53] Upon separating the AFM tip from the support, the C-terminal end of the BR molecule is stretched and a force builds up. As soon as the stretching force overcomes the stability of BR the structural segment directly connected to the C-terminal end unfolds. This unfolding step extends the polypeptide linking the pulling AFM tip and the portion of the BR molecule that remains folded and anchored in the membrane. Continuously withdrawing the AFM tip stretches the previously unfolded polypeptide until the forthcoming structural segment is loaded, mechanically stressed, and unfolded. The unfolding of structural segments forming stably folded entities continues until the entire BR molecule has been unfolded. This scenario explains that every single force peak of a F–D curve detects an unfolding intermediate of BR. The combination of all unfolding intermediates describes the unfolding pathway taken by the BR molecule.

BR in Purple Membrane and in Nanodiscs Choose Identical Unfolding Intermediates. Using SMFS we repeatedly unfolded single BR molecules that were embedded either in native purple membrane or in lipid nanodiscs under identical experimental conditions (Figure 2a,b; Methods). Every force peak of every F–D curve records an unfolding intermediate of BR that had certain probabilities to be detected.[28,53,55] An unfolding step describes the transition of one unfolding intermediate into the forthcoming one. Within such an unfolding step a structural segment of the BR molecule unfolds. The amplitude of a force peak quantifies the strength of the interaction that stabilizes a structural segment against unfolding. To visualize the common unfolding intermediates and steps of BR, we superimposed 100 F–D curves recorded of BR_{PM} (Figure 2c) and 100 F–D curves recorded of BR_{ND} (Figure 2d). Both superimpositions enhanced the force peaks that were common among all F–D curves.[53] The superimpositions of F–D curves recorded of BR_{PM} and BR_{ND} did not show any considerable differences.

We used the worm-like chain (WLC) model to fit every force peak (Methods) and to approximate the contour length of the stretched and unfolded BR polypeptide (Figure 2c,d). After having repeated this procedure for every force peak of every F–D curve we statistically analyzed the positions of all force peaks detected (Figure 3a,b). Histograms of the force peak positions detected for the unfolding of BR_{PM} and BR_{ND} showed minor differences. Student's *t*-tests revealed that none of these differences were statistically significant (Table 1). This suggests that the unfolding intermediates that were assigned by the force peaks did not differ from both preparations. We conclude that the stable structural segments forming the unfolding intermediates of BR did not depend on whether the membrane protein was embedded in the native purple membrane or in lipid nanodiscs.

We used the average contour lengths to assign the stable structural segments that established unfolding intermediates of the BR structure (Figure 4a,b). The contour length of every unfolding force peak (Figure 3) was used to assign the beginning of a stable structural segment and the end of the previously unfolded structural segment.[53] The stable structural segments detected for both BR_{PM} and BR_{ND} were similar to the segments repeatedly detected before, using native purple membrane.[24,28,56] This demonstrates that the unfolding intermediates shaping the unfolding pathway of BR in native purple membrane did not change upon reconstitution of BR into nanodiscs (Figure 4c).

Next we determined the average force of every unfolding force peak detected (Figure 3c,d). Histograms of the average unfolding forces showed minor differences between BR_{PM} and BR_{ND}, which were statistically not significant (Table 1). Because the average unfolding forces quantify the strength of interactions that stabilize the unfolding intermediates of BR, this comparison shows that the interactions established in BR did not depend on whether BR was embedded in the native purple membrane or in lipid nanodiscs. However, it cannot be excluded that more sensitive SMFS measurements in the future may allow detecting subtle differences.

BR_{PM} and BR_{ND} Populate Unfolding Intermediates Similarly. In the previous chapter we analyzed whether BR in native purple membrane and BR reconstituted in lipid nanodiscs show different unfolding intermediates and whether there is a difference in the interaction strengths stabilizing the individual unfolding intermediates. None of these analyses revealed significant differences. However, every unfolding intermediate occurred at a certain probability, and the sequence of unfolding intermediates describes a particular unfolding pathway taken by the BR molecule. To characterize whether BR in purple membrane and BR in lipid nanodiscs populate unfolding intermediates and pathways differently, we analyzed the probability for every unfolding intermediate that has been reproducibly taken by BR (Figure 4c; Table 1). The probability of every unfolding intermediate was obtained from the histogram providing the probability of single unfolding force peaks to be detected (Figure 3a,b). To determine the probability of a force peak described by a Gaussian distribution, we counted the number of F–D curves contributing a force peak to this distribution and divided it by the total number of F–D curves (Table 1).

The unfolding intermediates described by the unfolding force peaks at contour lengths of 23, 88, 148, and 219 aa were detected at a probability of 100%. Therefore, they were named main unfolding intermediates. Other unfolding intermediates of BR were detected at lower probability and were named minor unfolding intermediates. Thus, stressed at sufficiently high mechanical force the BR molecule always took the same main unfolding intermediates, whereas the minor unfolding intermediates were taken less frequently along the unfolding pathway. The probability of the less frequently occurring unfolding intermediates of BR_{ND} showed differences compared to those of BR_{PM} (Table 1). However, these differences and the number of F–D curves analyzed were too small to verify significance.[57]

From these results, we can conclude that, compared to BR of native purple membrane, the reconstitution into lipid nanodiscs did not cause BR to populate unfolding intermediates differently. To further investigate whether there is a difference in the minor unfolding intermediates of BR, more sensitive SMFS methods need to be established.

Limited Binding Probability of the C-Terminal End. The probability of attaching the C-terminal end of a BR molecule from purple membrane to the AFM tip was about 10 times higher (0.5%) compared to the probability of attaching the C-terminal end of a BR molecule

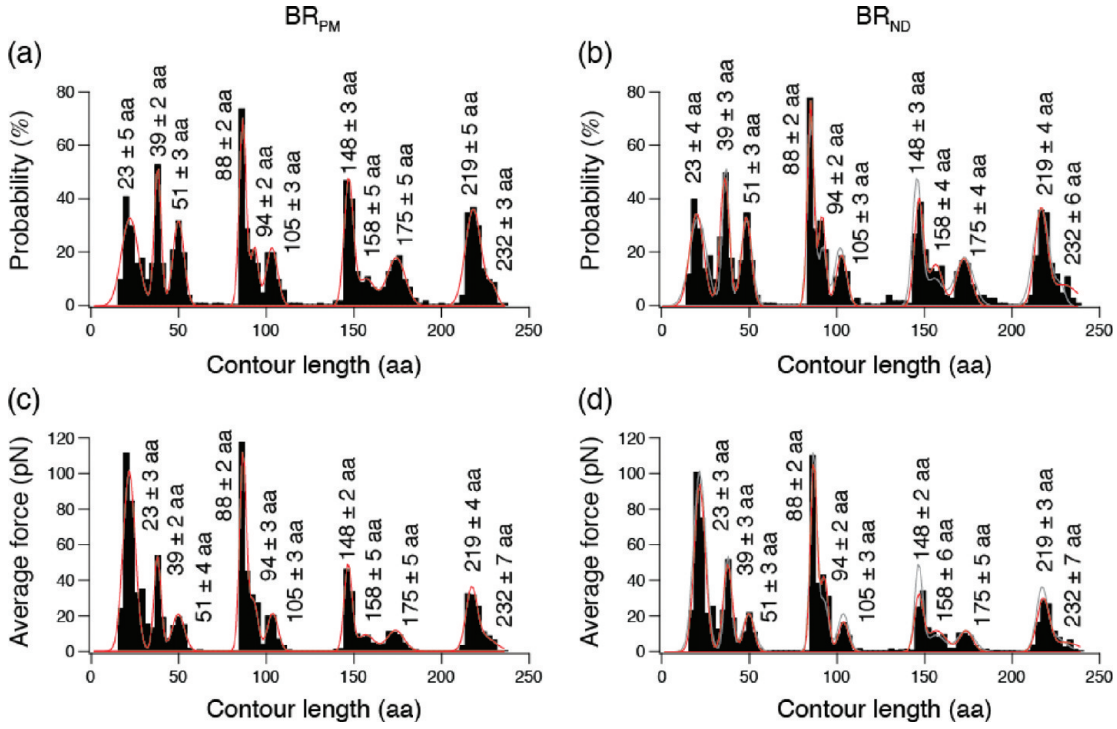

Figure 3. Probability and average force of unfolding intermediates of bacteriorhodopsin in native purple membrane (BR_{PM}) and of bacteriorhodopsin reconstituted in lipid nanodiscs (BR_{ND}). Probability of force peaks detected at certain contour lengths of BR_{PM} (a) and BR_{ND} (b). Average force of force peaks detected at certain contour lengths of BR_{PM} (c) and BR_{ND} (d). The contour length of every force peak of every F–D curve (n = 100 for each BR_{PM} and BR_{ND}) was determined by WLC fits (see Figure 2). Gaussian functions (red lines) were fitted to histograms to determine the average contour length of every peak including the standard deviation (fitted contour lengths in aa are given for every peak). Gray lines in (b) and (d) are Gaussian fits of the BR_{PM} reference data (a) and (c), respectively. Bin sizes of histograms were 3 aa. Student's t-tests did not reveal significant changes between BR_{PM} and BR_{ND} (Table 1).

TABLE 1. Unfolding Intermediates and Force Peak Probability of BR_{PM} and BR_{ND}[a]

		position of force peak (aa)			average force (pN)			probability (%)	
unfolding intermediate	localization of intermediate from N-terminal end (aa)	BR_{PM}	BR_{ND}	p-value	BR_{PM}	BR_{ND}	p-value	BR_{PM}	BR_{ND}
1	225	23 ± 5	23 ± 4	0.920	102 ± 28	94 ± 22	0.052	100	100
2	198	39 ± 2	39 ± 3	0.706	54 ± 15	49 ± 13	0.505	75	79
3	189	51 ± 3	51 ± 3	0.850	21 ± 7	22 ± 6	0.310	76	70
4	159	88 ± 2	88 ± 2	0.413	112 ± 18	105 ± 16	0.310	100	100
5	144	94 ± 2	94 ± 2	0.613	31 ± 5	42 ± 4	0.208	57	67
6	129	105 ± 3	105 ± 3	0.131	21 ± 3	16 ± 3	0.185	50	44
7	101	148 ± 3	148 ± 3	0.726	49 ± 4	33 ± 4	0.865	100	100
8	79	158 ± 5	158 ± 4	0.071	9 ± 3	12 ± 3	0.062	34	40
9	63	175 ± 5	175 ± 4	0.221	12 ± 3	12 ± 2	0.602	73	67
10	30	219 ± 5	219 ± 4	0.941	37 ± 5	30 ± 5	0.116	100	100
11	17	232 ± 3	232 ± 6	0.063	7 ± 3	5 ± 3	0.058	42	52

[a] Values given are averages and standard deviations (Figure 3). p-Values give the statistical difference in the force peak positions and average forces of BR_{PM} and BR_{ND} as determined by Student's t-tests. p-Values < 0.01 are considered significant.

in lipid nanodiscs (0.05%). Therefore, we had to conduct 10 times more experiments to obtain the 100 F–D curves from BR_{ND} in order to superimpose and analyze them in this work (Figures 2, 3). Revealing a statistically relevant number of F–D curves is mandatory to establish SMFS and dynamic force spectroscopy assays to characterize membrane proteins.[24,28,32,56,58,59] Thus, the low attachment rate of BR from nanodiscs to the AFM tip makes it challenging to obtain sufficient amounts of F–D curves. Several scenarios appear feasible to increase the number of F–D curves recorded from nanodiscs. Most probably the nanodisc preparation characterized for our measurements also contained empty lipid nanodiscs without inserted BR. To overcome this problem, recombinant BR with an affinity tag could be used to separate in a further purification step empty

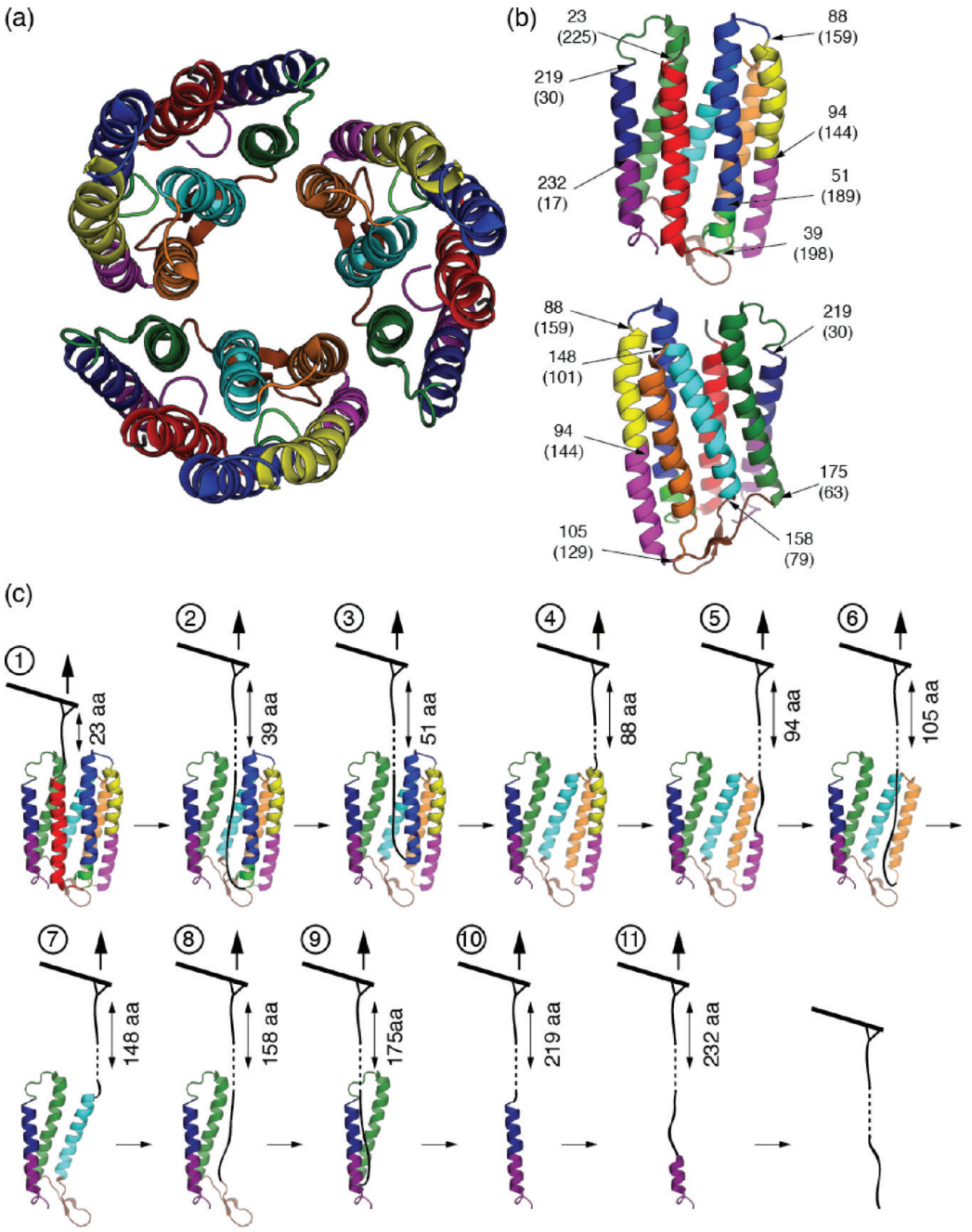

Figure 4. Stable structural segments that establish unfolding intermediates of bacteriorhodopsin. (a) Top view of the BR trimer from the cytoplasmic surface (PDB ID 1FFB). (b) Side view of the BR monomer. Numbers without brackets indicate the structural position (in aa) at which a force peak is assigned to the end of one stable structural stable segment and to the beginning of the forthcoming structural segment. Numbers in brackets denote the corresponding residue (in aa) in the BR sequence. Individual structural segments are equally colored. (c) Unfolding intermediates of BR. After attaching the AFM tip to the C-terminal end the retracting AFM cantilever induces the mechanical unfolding of the BR molecule. In a first step the C-terminal end is stretched (unfolding intermediate 1). At sufficiently high force the first unfolding step occurs and transfers unfolding intermediate 1 into the unfolding intermediate 2. Within this unfolding step the structural segment highlighted in red unfolds. Subsequent retraction of the cantilever stepwise unfolds the BR molecule and stretches the unfolded polypeptide (unfolding intermediates 2−10). In the last unfolding step the remainder of the BR molecule is extracted from the membrane. The sequence of unfolding steps describes the transition of one unfolding intermediate into the next one. The sequence of all unfolding intermediates describes the unfolding pathway taken by the BR molecule. As shown in Table 1 every unfolding intermediate of BR had a certain probability of occurring. In some cases, one or more unfolding intermediates unfolded collectively in one unfolding step.

nanodiscs from BR_{ND}. Furthermore, it is conceivable that in our preparation the nanodiscs adsorb onto the support with a random orientation (Figure S3, SI). Therefore, the functionalization of the support to favor a certain orientation of nanodiscs may increase the probability of the AFM tip to attach the terminal end of the membrane protein.

Orienting the nanodiscs may also help to reveal AFM topographs at sufficiently high resolution to identify single BR molecules in the nanodisc. In addition, elongating one of the terminal ends of the membrane protein may be helpful to improve the attachment rate to the AFM tip.

SUMMARY

In previous SMFS experiments we have investigated whether temperature, mutations, ions, oligomeric assembly, activation, or molecular compounds modify or establish interactions that initiate the formation of new (un)folding intermediates of membrane proteins embedded in their native lipid membrane.[24,26−31,60] So far none of these experiments detected that a membrane protein establishes a new unfolding intermediate or stable structural segment. These results suggest that the unfolding intermediates and thus the stable structural segments established within functional membrane proteins are conserved.[32,33] However, when changing external and internal factors modulating the functional state and stability of a membrane protein, it was observed that they can significantly change the probability of detecting certain unfolding intermediates by SMFS.[25−27,30,31] In most of these examples the probability of detecting an unfolding intermediate increased with the strength of the interaction stabilizing a particular structural segment. Thus, the interactions stabilizing structural segments within membrane proteins depend sensitively on the environment.

In our SMFS experiments we could not detect significant changes of the interaction strengths stabilizing structural segments (unfolding intermediates) of BR embedded in purple membrane and of BR embedded in lipid nanodiscs (Figure 3, Table 1). To some extent this finding may be considered surprising because the assembly of BR in purple membrane is quite different from BR in lipid nanodiscs (Figure 1). Although our phospholipid nanodiscs may contain residual lipids that have been coextracted with BR from purple membrane, the overall lipid composition of nanodiscs certainly differs from the lipid composition surrounding BR in the native purple membrane. However, as the UV/vis absorption spectrum of BR is sensitive to functional alterations,[49] the largely unchanged absorption spectrum suggests that the native structure and function relationship of BR was maintained upon reconstitution into phospholipid nanodiscs (Figure S1, SI). Because the functional characterization of BR_{PM} and BR_{ND} reveals no significant differences, one may infer that the inter- and intramolecular interactions within BR change very little. From this perspective it is not surprising that the SMFS experiments did not detect significant changes of interactions established for BR_{PM} and BR_{ND}. Biochemical and biophysical studies showed that BR molecules natively assembled into the BR trimer are structurally and thermally more stable compared to monomeric BR molecules.[28,61,62] Thus it can be assumed that the individual BR molecule is significantly stabilized by intermolecular interactions formed within the native BR trimer.

In our experiments we reconstituted the BR trimer into the lipid nanodiscs (Figure S2, SI) and did not observe significant changes of the folding, stability, and the interactions established in BR molecules. To what extent this effect may be attributed to the interactions stabilizing BR molecules within the BR trimer has to be shown. Although in our experiments the modified lipid environment of the nanodisc showed negligible influence on the function and stability of BR, this may not be generalized for other membrane proteins. Particularly, the lipid composition of membranes can functionally modulate membrane proteins.[35,63−65] Therefore, it may be too farfetched to conclude from our results that lipid nanodiscs do not change interactions of membrane proteins in general. It may be more realistic to conclude that SMFS of native membrane proteins can be conducted from lipid membranes and from lipid nanodiscs and that the composition of lipid nanodiscs must be chosen carefully to maintain the native stability, structure, and function of a particular membrane protein.

In our experiments we could not detect significant changes of the BR stability, unfolding intermediates, and unfolding pathways. We therefore conclude that membrane proteins can be reconstituted into lipid nanodiscs to study their stability and folding using single molecule techniques such as SMFS. One advantage of using nanodiscs to study membrane proteins by SMFS is that the reconstitution can be adjusted to specific conditions required to maintain the native structure and function relationship of the membrane protein. The main advantage of our approach is that membrane proteins reconstituted into nanodiscs can be handled with similar ease to water-soluble proteins. Most importantly, membrane proteins in nanodiscs can be prepared for SMFS and investigated by SMFS similar to water-soluble proteins. Consequently, high-resolution AFM imaging to localize membrane proteins is not required anymore for SMFS. This will enable performing high-throughput SMFS of membrane proteins in nanodiscs that homogeneously cover the SMFS support. Such high-throughput SMFS assays may allow screening for ligands or drugs that bind to the membrane protein of interest, *e.g.*, molecular transporters or G protein-coupled receptors.[25−27,30] Furthermore, membrane proteins might be sandwiched into polyprotein constructs[66] and characterized with advanced SMFS approaches that have been developed and established using water-soluble proteins. Such approaches include using instrumentations that have been developed to significantly improve force sensitivity,[67,68] time resolution,[69] throughput,[40,70,71] and thermal stability (drift)[72] of the SMFS experiment and that are less well

suited for high-resolution AFM imaging of biological samples. Taken together, lipid nanodiscs will open new doors for the characterization of membrane proteins by SMFS.

METHODS

Expression and Purification of MSP1. *Escherichia coli* BL21 star (DE3, Invitrogen, Germany) was transformed with the plasmid containing the membrane scaffold protein 1 (MSP1) gene (pET28b-MSP1). The MSP1 had an N-terminal 6-His affinity tag and a tobacco etch virus protease cleavage site.[10] A preculture was incubated overnight in lysogeny broth medium (supplemented with 30 μg/mL of kanamycin) and diluted 30-fold in expression media (lysogeny broth medium, supplemented with 0.5% (w/v) glucose and 30 μg/mL kanamycin). *E. coli* were grown at 37 °C with shaking (180 rpm). Expression of MSP1 was induced by adding isopropyl-β-D-thiogalactopyranoside to a final concentration of 1 mM when the optical density at λ = 600 nm (OD_{600}) reached 1. Subsequently, the cells were incubated under continuous shaking (180 rpm) for one hour at 37 °C before the temperature was decreased to 28 °C for an additional 4 h. Bacteria were pelleted and stored at −20 °C. Bacteria pellets of 1.2 L expression culture were resuspended in 50 mL of breaking buffer (300 mM NaCl, 1 protease inhibitor tablet (Complete Protease Inhibitor Cocktail Tablet, Roche, Germany), 1 mM phenylmethanesulfonylfuoride, 40 mM Tris-HCl, pH 8.0). Triton X-100 was added to a final concentration of 1% (v/v). Cells were disrupted using a Labsonic homogenizer (Braun, Germany) for 3 × 60 s and 3 × 45 s (pulse length 0.7 s) on ice. The suspension was centrifuged at 30.000*g* for 20 min to separate unbroken bacteria from bacteria debris. The supernatant was filtered (pore size 0.45 μm) before loading on an immobilized metal ion affinity chromatography column (IMAC Sepharose 6 FF, GE Healthcare, USA). The IMAC column was equilibrated with 5 column volumes of buffer 1 (300 mM NaCl, 40 mM Tris-HCl, 1% Triton-X100 (v/v), pH 8.0) before loading the supernatant. The column was washed successively with 5 column volumes of buffer 1 to 4 (buffer 2: 300 mM NaCl, 50 mM cholic acid, 40 mM Tris-HCl, pH 8.9; buffer 3: 300 mM NaCl, 40 mM Tris-HCl, pH 8.0; buffer 4: 300 mM NaCl, 50 mM imidazole, 40 mM Tris-HCl, pH 8.0) followed by the elution of MSP1 with elution buffer (300 mM NaCl, 300 mM imidazol, 40 mM Tris-HCl, pH 8.0). Purity of the elution fraction was analyzed by SDS-PAGE. MSP1-containing fractions were pooled, and glycerol was added to a final concentration of 10% (v/v) to prevent aggregation. MSP1 was dialyzed against dialysis buffer (300 mM NaCl, 40 mM Tris-HCl, 10% glycerol (v/v), pH 8.0) for 16 h at 4 °C with one buffer exchange. The dialysis was performed using Spectra/Por dialysis membranes with 10 kDa molecular weight cutoff (Spectrum Laboratories, USA). MSP1 concentration was determined by absorption spectroscopy using the molar extinction coefficient at λ = 280 nm (ε = 24 750 M^{-1} cm^{-1}). MSP1 was flash frozen in liquid nitrogen and stored at −80 °C.

Preparation of BR. Purple membrane from strain *H. salinarum* S9 was purified as described.[73] For reconstitution of BR into nanodiscs, purple membrane (concentration 4.5−6 mg/mL) was mixed with an equal volume of solubilization buffer (40 mM Na_2HPO_4/KH_2PO_4, 7.5% (w/v) *n*-octyl-β-D-glucopyranoside (Sigma-Aldrich, Germany), pH 6.9) and incubated at 4 °C for ≥2 days to extract BR from purple membrane. The solution was centrifuged at 90.000*g* for 1 h to remove insoluble fragments. The supernatant containing solubilized BR (including some tightly bound purple membrane lipids) was used for nanodisc reconstitution with the BR concentration being determined using the molar absorption coefficient at λ = 560 nm (ε = 42 000 M^{-1} cm^{-1}).

Reconstitution of BR into Nanodiscs. Dimyristoylphosphatidylcholine (Avanti Polar Lipids, USA) was added to water at a concentration of 50 mM and solubilized by adding sodium cholate to a final concentration of 100 mM. The detergent−lipid mixture was sonicated for 10 min at 35 kHz and 640 W in a water bath (Sonorex Super RK 510, Bandelin, Germany) and filtered (pore size 0.45 μm). BR was reconstituted into nanodiscs by mixing detergent-solubilized BR with MSP1 and DMPC at a stoichiometry of 1:1:10 (molar ratio). The BR-MSP1-DMPC mixture was incubated for 1 h at room temperature (~23 °C). To remove detergent and to induce nanodisc formation, the mixture was dialyzed overnight at room temperature against detergent-free buffer (100 mM NaCl, 10 mM Tris, pH 7.4) at a ratio of ≥1:500. Since no purification step was performed after solubilization of BR, the nanodiscs also contained wild-type lipids from purple membrane. The following dialysis was performed at 4 °C for additional 2 days. The detergent-free buffer was exchanged at least twice. Avoid photobleaching of BR,[74] all reconstitution procedures were carried out in the dark. After dialysis the aggregated material was removed by centrifugation at 22.000*g* for 20 min. The supernatant was concentrated using Amicon ultracentrifugal filter units (Millipore, Germany, 10 kDa molecular weight cutoff) to a final volume of 0.5 mL. BR_{ND} complexes were purified using size-exclusion chromatography (Superdex 200, Tricorn 10/300, GE Healthcare, Germany) using detergent-free buffer. Elution fractions with absorption maxima at λ = 560 nm were pooled and concentrated using ultracentrifugal filter units (Amicon, 10 kDa molecular weight cutoff) to a final concentration of ~100 μM. Finally, the sample was centrifuged (20 min at 22.000*g*). The supernatant was stored at 4 °C until analysis.

SMFS. AFM imaging of BR_{PM} and BR_{ND} (Figure S3, SI) was performed using a Nanowizard II (JPK Instruments, Germany) and a Multimode8 AFM (Bruker, Germany). SMFS on BR_{PM} was conducted using a NanoWizard II (JPK Instruments), whereas BR_{ND} was approached using a ForceRobot 300 (JPK Instruments). The rectangular, 200 μm long AFM cantilevers (OMCL-RC800PSA, Olympus, Japan) having a nominal spring constant of ~0.05 N/m were calibrated in buffer solution using the equipartition theorem.[75,76] Spring constants determined were within ~10% of each other. Experiments were carried out using AFM cantilevers from the same wafer. To nonspecifically attach the AFM tip to BR, the tip was pushed against the purple membrane or BR_{ND} applying a force of ~1 nN for 1 s.[28,37] Subsequent retraction of the AFM cantilever induced a mechanical load that unfolded BR. While retracting the AFM cantilever at a velocity of 528 nm/s, the cantilever deflection was recorded to measure the force with dependence on the pulling distance. To record F−D curves, a raster of several hundred spots was defined. One F−D curve was recorded for every spot. In purple membrane the distance between adjacent BR trimers corresponds to ~6.2 nm.[41−44] To ensure that single BR monomers were unfolded from intact BR trimers, the separation between adjacent spots was set at ~20 nm for purple membrane. To ensure that only one F−D curve per nanodisc was recorded, the distance between adjacent spots was set at >50 nm for BR_{ND}. All SMFS experiments were performed using identical buffer solution (150 mM KCl, 20 mM Tris-HCl, pH 8.0) at room temperature.

Selection and Analysis of F−D Curves. First we selected F−D curves exhibiting an overall length between 60 and 70 nm, since they represented the complete unfolding of a BR into a fully stretched conformation.[37] Then we selected F−D curves that corresponded to the C-terminal unfolding of BR.[37,54] All F−D curves were aligned using the characteristic force peak at a contour length of 88 amino acids as reference. Every force peak of a F−D curve was fitted using the WLC model,

$$F(x) = \frac{k_B T}{P}\left[0.25\left(1-\frac{x}{L}\right)^{-2} - 0.25 + \frac{x}{L}\right]$$

where P is the persistence length of an amino acid (0.4 nm), x the AFM tip−sample distance (extension of the unfolded and fully stretched polypeptide), k_B the Boltzmann constant, and T the temperature.[37] The contour length L of the unfolded and fully stretched polypeptide was obtained from fitting a force peak

using the WLC model. Division of L by the length of an amino acid (0.36 nm) reveals the number of unfolded and stretched amino acids. The amplitude of a force peak denotes the strength of interactions that stabilized a structural segment against unfolding. Every force peak of every F–D curve was analyzed to quantify contour length and unfolding force (Figure 3). To determine the average force shown in histograms (Figure 3), the average force of a particular force peak was calculated and multiplied by its probability of detection. This procedure gives the average force of an unfolding force peak from all unfolding F–D curves analyzed.

Assignment of Stable Structural Segments. The contour length determined using the WLC model corresponds to the length of the unfolded and stretched BR polypeptide that tethers the AFM tip and a structural unfolding intermediate. Thus, each force peak was used to assign the end of the previous and the beginning of the following structural segment that stabilized BR against unfolding.[22] Some stable structural segments had to be assumed to end or begin at the periplasmic BR surface opposite side to the pulling AFM tip. Therefore, the so-called "membrane compensation procedure" was applied to correct the contour lengths.[22,53] To locate such a beginning of a stable structural segment, the thickness of the membrane (~4 nm) was added to the contour length of the corresponding force peak. Accordingly, ~11 aa (4 nm/0.36 nm/aa) were added to the contour length of a force peak. If the beginning of a stable structural segment occurred within the membrane, fewer aa were added to the contour length to locate the beginning of the stable structural segment in the membrane.

Acknowledgment. The European Community's Seventh Framework Programme ([FP7/2007-2013] under grant agreement no. 211800) and the Deutsche Forschungsgemeinschaft supported this work. We thank C. Bippes for assistance and for critical reading of the manuscript and G. Büldt for kindly providing purple membrane.

Supporting Information Available: UV/vis spectra of BR_{ND} and BR_{PM}, circular dichroism spectra of BR_{ND}, and AFM topographs of purple membrane and nanodiscs (BR_{ND}). This material is available free of charge *via* the Internet at http://pubs.acs.org.

REFERENCES AND NOTES

1. Alberts, B.; Johnson, A.; Lewis, J.; Raff, M.; Roberts, K.; Walter, P. Membrane Proteins. In *Molecular Biology of the Cell*; Anderson, M., Granum, S., Eds.; Taylor and Francis: New York, 2007; pp 629–649.
2. Wallin, E.; von Heijne, G. Genome-Wide Analysis of Integral Membrane Proteins from Eubacterial, Archaean, and Eukaryotic Organisms. *Protein Sci.* **1998**, *7*, 1029–1038.
3. Dill, K. A.; Chan, H. S. From Levinthal to Pathways to Funnels. *Nat. Struct. Biol.* **1997**, *4*, 10–19.
4. White, S. H.; Wimley, W. C. Membrane Protein Folding and Stability: Physical Principles. *Annu. Rev. Biophys. Biomol. Struct.* **1999**, *28*, 319–365.
5. Bowie, J. U. Solving the Membrane Protein Folding Problem. *Nature* **2005**, *438*, 581–589.
6. Engelman, D. M. Membranes Are More Mosaic Than Fluid. *Nature* **2005**, *438*, 578–580.
7. Lingwood, D.; Simons, K. Lipid Rafts as a Membrane-Organizing Principle. *Science* **2010**, *327*, 46–50.
8. Bayburt, T. H.; Grinkova, Y. V.; Sligar, S. G. Self-Assembly of Discoidal Phospholipid Bilayer Nanoparticles with Membrane Scaffold Proteins. *Nano Lett.* **2002**, *2*, 853–856.
9. Sligar, S. G. Finding a Single-Molecule Solution for Membrane Proteins. *Biochem. Biophys. Res. Commun.* **2003**, *312*, 115–119.
10. Denisov, I. G.; Grinkova, Y. V.; Lazarides, A. A.; Sligar, S. G. Directed Self-Assembly of Monodisperse Phospholipid Bilayer Nanodiscs with Controlled Size. *J. Am. Chem. Soc.* **2004**, *126*, 3477–3487.
11. Boldog, T.; Grimme, S.; Li, M.; Sligar, S. G.; Hazelbauer, G. L. Nanodiscs Separate Chemoreceptor Oligomeric States and Reveal Their Signaling Properties. *Proc. Natl. Acad. Sci. U. S. A.* **2006**, *103*, 11509–11514.
12. Bayburt, T. H.; Sligar, S. G. Single-Molecule Height Measurements on Microsomal Cytochrome P450 in Nanometer-Scale Phospholipid Bilayer Disks. *Proc. Natl. Acad. Sci. U. S. A.* **2002**, *99*, 6725–6730.
13. Alami, M.; Dalal, K.; Lelj-Garolla, B.; Sligar, S. G.; Duong, F. Nanodiscs Unravel the Interaction between the SecYEG Channel and Its Cytosolic Partner SecA. *EMBO J.* **2007**, *26*, 1995–2004.
14. Bayburt, T. H.; Sligar, S. G. Self-Assembly of Single Integral Membrane Proteins into Soluble Nanoscale Phospholipid Bilayers. *Protein Sci.* **2003**, *12*, 2476–2481.
15. Leitz, A. J.; Bayburt, T. H.; Barnakov, A. N.; Springer, B. A.; Sligar, S. G. Functional Reconstitution of Beta2-Adrenergic Receptors Utilizing Self-Assembling Nanodisc Technology. *BioTechniques* **2006**, *40*, 601–602, 604, 606..
16. Whorton, M. R.; Bokoch, M. P.; Rasmussen, S. G.; Huang, B.; Zare, R. N.; Kobilka, B.; Sunahara, R. K. A Monomeric G Protein-Coupled Receptor Isolated in a High-Density Lipoprotein Particle Efficiently Activates Its G Protein. *Proc. Natl. Acad. Sci. U. S. A.* **2007**, *104*, 7682–7687.
17. Bayburt, T. H.; Vishnivetskiy, S. A.; McLean, M. A.; Morizumi, T.; Huang, C. C.; Tesmer, J. J.; Ernst, O. P.; Sligar, S. G.; Gurevich, V. V. Monomeric Rhodopsin Is Sufficient for Normal Rhodopsin Kinase (GRK1) Phosphorylation and Arrestin-1 Binding. *J. Biol. Chem.* **2011**, *286*, 1420–1428.
18. Kijac, A. Z.; Li, Y.; Sligar, S. G.; Rienstra, C. M. Magic-Angle Spinning Solid-State NMR Spectroscopy of Nanodisc-Embedded Human CYP3A4. *Biochemistry* **2007**, *46*, 13696–13703.
19. Raschle, T.; Hiller, S.; Yu, T. Y.; Rice, A. J.; Walz, T.; Wagner, G. Structural and Functional Characterization of the Integral Membrane Protein VDAC-1 in Lipid Bilayer Nanodiscs. *J. Am. Chem. Soc.* **2009**, *131*, 17777–17779.
20. Kijac, A.; Shih, A. Y.; Nieuwkoop, A. J.; Schulten, K.; Sligar, S. G.; Rienstra, C. M. Lipid-Protein Correlations in Nanoscale Phospholipid Bilayers Determined by Solid-State Nuclear Magnetic Resonance. *Biochemistry* **2010**, *49*, 9190–9198.
21. Borch, J.; Roepstorff, P.; Moller-Jensen, J. Nanodisc-Based Co-Immunoprecipitation for Mass Spectrometric Identification of Membrane-Interacting Proteins. *Mol. Cell. Proteomics* **2011**, *10*, O110–006775.
22. Kedrov, A.; Janovjak, H.; Sapra, K. T.; Muller, D. J. Deciphering Molecular Interactions of Native Membrane Proteins by Single-Molecule Force Spectroscopy. *Annu. Rev. Biophys. Biomol. Struct.* **2007**, *36*, 233–260.
23. Engel, A.; Gaub, H. E. Structure and Mechanics of Membrane Proteins. *Annu. Rev. Biochem.* **2008**, *77*, 127–148.
24. Janovjak, H.; Kessler, M.; Oesterhelt, D.; Gaub, H.; Muller, D. J. Unfolding Pathways of Native Bacteriorhodopsin Depend on Temperature. *EMBO J.* **2003**, *22*, 5220–5229.
25. Kedrov, A.; Krieg, M.; Ziegler, C.; Kuhlbrandt, W.; Muller, D. J. Locating Ligand Binding and Activation of a Single Antiporter. *EMBO Rep.* **2005**, *6*, 668–674.
26. Park, P. S.; Sapra, K. T.; Kolinski, M.; Filipek, S.; Palczewski, K.; Muller, D. J. Stabilizing Effect of Zn^{2+} in Native Bovine Rhodopsin. *J. Biol. Chem.* **2007**, *282*, 11377–11385.
27. Ge, L.; Perez, C.; Waclawska, I.; Ziegler, C.; Muller, D. J. Locating an Extracellular K^{+}-Dependent Interaction Site That Modulates Betaine-Binding of the Na^{+}-Coupled Betaine Symporter BetP. *Proc. Natl. Acad. Sci. U. S. A.* **2011**, *108*, E890–898.
28. Sapra, K. T.; Besir, H.; Oesterhelt, D.; Muller, D. J. Characterizing Molecular Interactions in Different Bacteriorhodopsin Assemblies by Single-Molecule Force Spectroscopy. *J. Mol. Biol.* **2006**, *355*, 640–650.
29. Kedrov, A.; Appel, M.; Baumann, H.; Ziegler, C.; Muller, D. J. Examining the Dynamic Energy Landscape of an Antiporter Upon Inhibitor Binding. *J. Mol. Biol.* **2008**, *375*, 1258–1266.
30. Bippes, C. A.; Zeltina, A.; Casagrande, F.; Ratera, M.; Palacin, M.; Muller, D. J.; Fotiadis, D. Substrate Binding Tunes Conformational Flexibility and Kinetic Stability of an Amino Acid Antiporter. *J. Biol. Chem.* **2009**, *284*, 18651–18663.
31. Kedrov, A.; Hellawell, A. M.; Klosin, A.; Broadhurst, R. B.; Kunji, E. R.; Muller, D. J. Probing the Interactions of

Carboxy-Atractyloside and Atractyloside with the Yeast Mitochondrial ADP/ATP Carrier. *Structure* **2010**, *18*, 39–46.
32. Sapra, K. T.; Balasubramanian, G. P.; Labudde, D.; Bowie, J. U.; Muller, D. J. Point Mutations in Membrane Proteins Reshape Energy Landscape and Populate Different Unfolding Pathways. *J. Mol. Biol.* **2008**, *376*, 1076–1090.
33. Sapra, K. T.; Doehner, J.; Renugopalakrishnan, V.; Padros, E.; Muller, D. J. Role of Extracellular Glutamic Acids in the Stability and Energy Landscape of Bacteriorhodopsin. *Biophys. J.* **2008**, *95*, 3407–3418.
34. Cisneros, D. A.; Oberbarnscheidt, L.; Pannier, A.; Klare, J. P.; Helenius, J.; Engelhard, M.; Oesterhelt, F.; Muller, D. J. Transducer Binding Establishes Localized Interactions to Tune Sensory Rhodopsin II. *Structure* **2008**, *16*, 1206–1213.
35. Opekarova, M.; Tanner, W. Specific Lipid Requirements of Membrane Proteins--a Putative Bottleneck in Heterologous Expression. *Biochim. Biophys. Acta* **2003**, *1610*, 11–22.
36. Seddon, A. M.; Curnow, P.; Booth, P. J. Membrane Proteins, Lipids and Detergents: Not Just a Soap Opera. *Biochim. Biophys. Acta* **2004**, *1666*, 105–117.
37. Oesterhelt, F.; Oesterhelt, D.; Pfeiffer, M.; Engel, A.; Gaub, H. E.; Muller, D. J. Unfolding Pathways of Individual Bacteriorhodopsins. *Science* **2000**, *288*, 143–146.
38. Muller, D. J.; Amrein, M.; Engel, A. Adsorption of Biological Molecules to a Solid Support for Scanning Probe Microscopy. *J. Struct. Biol.* **1997**, *119*, 172–188.
39. Bosshart, P. D.; Casagrande, F.; Frederix, P. L.; Ratera, M.; Bippes, C. A.; Muller, D. J.; Palacin, M.; Engel, A.; Fotiadis, D. High-Throughput Single-Molecule Force Spectroscopy for Membrane Proteins. *Nanotechnology* **2008**, *19*, 384014.
40. Struckmeier, J.; Wahl, R.; Leuschner, M.; Nunes, J.; Janovjak, H.; Geisler, U.; Hofmann, G.; Jahnke, T.; Muller, D. J. Fully Automated Single-Molecule Force Spectroscopy for Screening Applications. *Nanotechnology* **2008**, *19*, 384020.
41. Haupts, U.; Tittor, J.; Oesterhelt, D. Closing in on Bacteriorhodopsin: Progress in Understanding the Molecule. *Annu. Rev. Biophys. Biomol. Struct.* **1999**, *28*, 367–399.
42. Dencher, N. A.; Sass, H. J.; Buldt, G. Water and Bacteriorhodopsin: Structure, Dynamics, and Function. *Biochim. Biophys. Acta* **2000**, *1460*, 192–203.
43. Cartailler, J. P.; Luecke, H. X-Ray Crystallographic Analysis of Lipid-Protein Interactions in the Bacteriorhodopsin Purple Membrane. *Annu. Rev. Biophys. Biomol. Struct.* **2003**, *32*, 285–310.
44. Hirai, T.; Subramaniam, S.; Lanyi, J. K. Structural Snapshots of Conformational Changes in a Seven-Helix Membrane Protein: Lessons from Bacteriorhodopsin. *Curr. Opin. Struct. Biol.* **2009**, *19*, 433–439.
45. Huang, K. S.; Bayley, H.; Liao, M. J.; London, E.; Khorana, H. G. Refolding of an Integral Membrane Protein. Denaturation, Renaturation, and Reconstitution of Intact Bacteriorhodopsin and Two Proteolytic Fragments. *J. Biol. Chem.* **1981**, *256*, 3802–3809.
46. Brouillette, C. G.; Muccio, D. D.; Finney, T. K. pH Dependence of Bacteriorhodopsin Thermal Unfolding. *Biochemistry* **1987**, *26*, 7431–7438.
47. Popot, J. L.; Gerchman, S. E.; Engelman, D. M. Refolding of Bacteriorhodopsin in Lipid Bilayers. A Thermodynamically Controlled Two-Stage Process. *J. Mol. Biol.* **1987**, *198*, 655–676.
48. Engelman, D. M.; Chen, Y.; Chin, C. N.; Curran, A. R.; Dixon, A. M.; Dupuy, A. D.; Lee, A. S.; Lehnert, U.; Matthews, E. E.; Reshetnyak, Y. K.; *et al*. Membrane Protein Folding: Beyond the Two Stage Model. *FEBS Lett.* **2003**, *555*, 122–125.
49. Rehorek, M.; Heyn, M. P. Binding of All-Trans-Retinal to the Purple Membrane. Evidence for Cooperativity and Determination of the Extinction Coefficient. *Biochemistry* **1979**, *18*, 4977–4983.
50. Heyn, M. P.; Cherry, R. J.; Dencher, N. A. Lipid--Protein Interactions in Bacteriorhodopsin--Dimyristoylphosphatidylcholine Vesicles. *Biochemistry* **1981**, *20*, 840–849.
51. Isenbarger, T. A.; Krebs, M. P. Thermodynamic Stability of the Bacteriorhodopsin Lattice as Measured by Lipid Dilution. *Biochemistry* **2001**, *40*, 11923–11931.
52. Bayburt, T. H.; Grinkova, Y. V.; Sligar, S. G. Assembly of Single Bacteriorhodopsin Trimers in Bilayer Nanodiscs. *Arch. Biochem. Biophys.* **2006**, *450*, 215–222.
53. Muller, D. J.; Kessler, M.; Oesterhelt, F.; Moller, C.; Oesterhelt, D.; Gaub, H. Stability of Bacteriorhodopsin Alpha-Helices and Loops Analyzed by Single-Molecule Force Spectroscopy. *Biophys. J.* **2002**, *83*, 3578–3588.
54. Kessler, M.; Gaub, H. E. Unfolding Barriers in Bacteriorhodopsin Probed from the Cytoplasmic and the Extracellular Side by AFM. *Structure* **2006**, *14*, 521–527.
55. Janovjak, H.; Struckmeier, J.; Hubain, M.; Kedrov, A.; Kessler, M.; Muller, D. J. Probing the Energy Landscape of the Membrane Protein Bacteriorhodopsin. *Structure* **2004**, *12*, 871–879.
56. Sapra, K. T.; Park, P. S.; Palczewski, K.; Muller, D. J. Mechanical Properties of Bovine Rhodopsin and Bacteriorhodopsin: Possible Roles in Folding and Function. *Langmuir* **2008**, *24*, 1330–1337.
57. Dufrene, Y. F.; Evans, E.; Engel, A.; Helenius, J.; Gaub, H. E.; Muller, D. J. Five Challenges to Bringing Single-Molecule Force Spectroscopy into Living Cells. *Nat. Methods* **2011**, *8*, 123–127.
58. Sapra, K. T.; Park, P. S. H.; Filipek, S.; Engel, A.; Muller, D. J.; Palczewski, K. Detecting Molecular Interactions That Stabilize Native Bovine Rhodopsin. *J. Mol. Biol.* **2006**, *358*, 255–269.
59. Janovjak, H.; Sapra, K. T.; Kedrov, A.; Muller, D. J. From Valleys to Ridges: Exploring the Dynamic Energy Landscape of Single Membrane Proteins. *ChemPhysChem* **2008**, *9*, 954–966.
60. Damaghi, M.; Bippes, C.; Koster, S.; Yildiz, O.; Mari, S. A.; Kuhlbrandt, W.; Muller, D. J. pH-Dependent Interactions Guide the Folding and Gate the Transmembrane Pore of the Beta-Barrel Membrane Protein OmpG. *J. Mol. Biol.* **2010**, *397*, 878–882.
61. Brouillette, C. G.; McMichens, R. B.; Stern, L. J.; Khorana, H. G. Structure and Thermal Stability of Monomeric Bacteriorhodopsin in Mixed Phospholipid/Detergent Micelles. *Proteins* **1989**, *5*, 38–46.
62. Heyes, C. D.; El-Sayed, M. A. The Role of the Native Lipids and Lattice Structure in Bacteriorhodopsin Protein Conformation and Stability as Studied by Temperature-Dependent Fourier Transform-Infrared Spectroscopy. *J. Biol. Chem.* **2002**, *277*, 29437–29443.
63. Lee, A. G. How Lipids Affect the Activities of Integral Membrane Proteins. *Biochim. Biophys. Acta* **2004**, *1666*, 62–87.
64. Hunte, C. Specific Protein-Lipid Interactions in Membrane Proteins. *Biochem. Soc. Trans.* **2005**, *33*, 938–942.
65. Hunte, C.; Richers, S. Lipids and Membrane Protein Structures. *Curr. Opin. Struct. Biol.* **2008**, *18*, 406–411.
66. Rief, M.; Pascual, J.; Saraste, M.; Gaub, H. E. Single Molecule Force Spectroscopy of Spectrin Repeats: Low Unfolding Forces in Helix Bundles. *J. Mol. Biol.* **1999**, *286*, 553–561.
67. Stahl, S. W.; Puchner, E. M.; Gaub, H. E. Photothermal Cantilever Actuation for Fast Single-Molecule Force Spectroscopy. *Rev. Sci. Instrum.* **2009**, *80*, 073702.
68. Kobayashi, K.; Yamada, H.; Matsushige, K. Reduction of Frequency Noise and Frequency Shift by Phase Shifting Elements in Frequency Modulation Atomic Force Microscopy. *Rev. Sci. Instrum.* **2011**, *82*, 033702.
69. Sahin, O.; Magonov, S.; Su, C.; Quate, C. F.; Solgaard, O. An Atomic Force Microscope Tip Designed to Measure Time-Varying Nanomechanical Forces. *Nat. Nanotechnol.* **2007**, *2*, 507–514.
70. Lang, H. P.; Hegner, M.; Gerber, C. Cantilever Array Sensors. *Mater. Today* **2005**, *8*, 30–36.
71. Favre, M.; Polesel-Maris, J.; Overstolz, T.; Niedermann, P.; Dasen, S.; Gruener, G.; Ischer, R.; Vettiger, P.; Liley, M.; Heinzelmann, H.; *et al*. Parallel AFM Imaging and Force Spectroscopy Using Two-Dimensional Probe Arrays for Applications in Cell Biology. *J. Mol. Recognit.* **2011**, *24*, 446–452.
72. King, G. M.; Carter, A. R.; Churnside, A. B.; Eberle, L. S.; Perkins, T. T. Ultrastable Atomic Force Microscopy: Atomic-Scale

Stability and Registration in Ambient Conditions. *Nano Lett.* **2009**, *9*, 1451–1456.
73. Oesterhelt, D.; Stoeckenius, W. Isolation of the Cell Membrane of Halobacterium Halobium and Its Fractionation into Red and Purple Membrane. *Methods Enzymol.* **1974**, *31*, 667–678.
74. Mukai, Y.; Kamo, N.; Mitaku, S. Light-Induced Denaturation of Bacteriorhodopsin Solubilized by Octyl-Beta-Glucoside. *Protein Eng.* **1999**, *12*, 755–759.
75. Florin, E. L.; Rief, M.; Lehmann, H.; Ludwig, Dornmair, C.; Moy, V. T.; Gaub, H. E. Sensing Specific Molecular-Interactions with the Atomic-Force Microscope. *Biosens. Bioelectron.* **1995**, *10*, 895–901.
76. Butt, H.-J.; Jaschke, M. Calculation of Thermal Noise in Atomic Force Microscopy. *Nanotechnol.* **1995**, *6*, 1–7.